AIAA 2002-3917

Engine Cycle and Exhaust Configurations for Quiet Supersonic Propulsion

D. Papamoschou
Dept. of Mechanical & Aerospace Engineering
University of California at Irvine
Irvine, CA

38th AIAA/ASME/SAE/ASEE
Joint Propulsion Conference & Exhibit
7-10 July 2002
Indianapolis, Indiana

AIAA-2002-3917

ENGINE CYCLE AND EXHAUST CONFIGURATIONS FOR QUIET SUPERSONIC PROPULSION

Dimitri Papamoschou *
University of California, Irvine, Irvine, California 92697-3975

This study explores the thermodynamics and acoustics of a fixed-cycle, bypass ratio 3 supersonic engine with an innovative noise suppression scheme. The silencing method entails installation of turning vanes in the bypass exhaust of a separate-flow turbofan engine. The vanes produce locally-skewed mixing layers between the core and bypass flows and give a slight downward tilt to the bypass plume relative to the core plume. The former effect reduces the length of the core noise source region and the latter effect thickens the bypass stream on the underside of the jet. This results in a reduction of the convective Mach number of instability waves that produce intense downward sound radiation. Subscale experiments show a substantial noise benefit. Relative to the mixed-flow exhaust, the coaxial separate-flow exhaust with vanes reduces the peak overall sound pressure level by 8 dB and the effective perceived noise level by 7 dB. The noise-equivalent specific thrust on takeoff is reduced from 490 m/s to 390 m/s. Compared to a current-generation low-bypass turbofan engine, the bypass ratio 3 engine is estimated to be 13-dB quieter with the mixed-flow exhaust and 20-dB quieter with the aforementioned suppression scheme.

Nomenclature

D	=	diameter or drag
f	=	frequency
$\dot{m}$	=	mass flow rate
M	=	Mach number
U	=	velocity
r	=	distance from jet exit
t	=	time from lift off
$\mathcal{T}$	=	thrust
x	=	horizontal distance from brake release
y	=	altitude
α	=	geometric angle of attack
γ	=	climb angle
θ	=	polar angle relative to jet centerline
ϕ	=	azimuth angle relative to vertical plane
ψ	=	polar observation angle of airplane

Subscripts

com	=	compressor
eng	=	full-scale engine
exp	=	subscale experiment
fan	=	fan tip
LO	=	lift off
p	=	primary (core) exhaust
s	=	secondary (bypass) exhaust
TOM	=	takeoff monitor
tot	=	total
∞	=	flight conditions

Abbreviations

BPR	=	Bypass Ratio
EPNL	=	Effective Perceived Noise Level
FPR	=	Fan Pressure Ratio
PNL	=	Perceived Noise Level
PNLM	=	Maximum value of PNL
SPL	=	Sound Pressure Level
OASPL	=	Overall Sound Pressure Level
OPR	=	Overall Pressure Ratio
TIT	=	Turbine Inlet Temperature
TSFC	=	Thrust Specific Fuel Consumption

*Professor, Associate Fellow AIAA

** Noise suppression via deflection of the bypass and/or core streams is proprietary to the University of California. U.S. Patent Pending.

Introduction

Development of large-scale supersonic transportation has been a long-sought and elusive goal for the aerospace industry. The efficiency and environmental compliance of a viable supersonic airplane should be on a par with those of advanced subsonic aircraft. Environmental problems include emissions, sonic boom, and takeoff noise. The latter has been the subject of intense research and development for over forty years, which has led to significant progress in our understanding and prediction of jet noise. A large variety of noteworthy suppression schemes were proposed and investigated. However, the problem today remains as challenging as it was forty years ago [1].

At the heart of the issue are the conflicting requirements for an engine that is both quiet on takeoff and efficient at supersonic cruise. Quiet takeoff requires low specific thrust (high mass flow rate). Efficient supersonic cruise entails high specific thrust (low mass flow rate), primarily to minimize the frontal area of the engine. In an effort to resolve this conflict, past efforts have investigated engines with variable-geometry ejectors [2] as well as turbofan engines with variable cycle (variable bypass ratio). These concepts are notable and are still being pursued but, at present, entail complexity far greater than that of today's commercial engines.

An ideal concept, of course, would be a fixed-cycle engine that is quiet on takeoff and efficient at cruise. While this idea was probably unfeasible several years ago, advances in engine technology bring it closer to reality today. A key parameter is the turbine inlet temperature (TIT). As will be shown in the next section, increasing TIT allows a supersonic engine to operate at higher bypass ratio while maintaining a reasonably small frontal area. Of course, the bypass ratio will never reach the values found in modern subsonic engines, which range from five to nine. Reasonable values for supersonic engines are in the ballpark of two to three; higher values would lead to prohibitively large frontal areas.

This means that noise is still an issue as the supersonic engine on takeoff will have higher specific thrust than its subsonic counterparts. Can an an aircraft powered by engines with bypass ratio three become as quiet as one powered by engines with bypass ratio eight? The complete answer requires a systems-level view that, at a minimum, considers the following basic and interdependent elements: (a) engine cycle; (b) exhaust configuration; (c) *perceived* noise (as opposed to absolute noise); and (d) aircraft performance. It is conceivable that optimization at the systems level, and implementation of non-traditional exhaust concepts, will lead to a very quiet airplane even though the engine has higher specific thrust than its subsonic counterparts.

This study looks at the above four elements, with emphasis on the effect of exhaust configuration. Given that the bypass ratio is moderate, it becomes crucial how one uses the bypass stream to reduce noise. One arrangement is the mixed-flow exhaust, currently used on all military engines, in which the bypass and core streams mix before exiting a common nozzle. The other option is the separate (unmixed)-flow turbofan, which is very common on subsonic transports. The unmixed design allows shaping of the bypass exhaust so that the bypass stream "shields" noise emitted from the core stream. Past work on a BPR=1.6 supersonic engine [3] has demonstrated the substantial noise benefit of eccentric separate-flow nozzles. Most recently, alternatives to the eccentric arrangement were developed that make the exhaust arrangement even simpler and allow online control of noise suppression [4]. This paper extends the BPR=1.6 work to BPR=3.0 and assesses the impact of the new nozzle configurations.

Engine Cycle

Advances in turbine technology will soon allow steady-state (cruise) operation at turbine inlet temperatures around 1800-1900°K. This means that more power will be available to drive a fan with bypass ratio larger than those traditionally used in supersonic turbofan engines (0.5 or less.) Large bypass ratio is desired for quiet takeoff but increases the frontal area of the engine, which is undesirable for supersonic operation. However, at constant thrust, bypass ratio, and fan pressure ratio, the fan diameter decreases with increasing TIT. Figure 1 plots the variation of fan diameter and thrust specific fuel consumption versus TIT at Mach 1.6 cruise for an engine with BPR=3.0 and FPR=2.2. The plots are based an a cycle analysis described later in this section. There is clearly a very significant benefit of a reduced frontal area with increasing TIT. For the conditions shown on the plot, the TSFC has a minimum around TIT=1800°K. So a cruise setting of TIT=1800°K seems to be a reasonable design point.

Given a turbine inlet temperature in the neighbor-

Table 1: Engine Cycle Assumptions

Component	Efficiency	Specific heat ratio
Inlet ($M_\infty < 1$)	0.97	1.40
Inlet ($M_\infty \geq 1$)	0.85	1.40
Fan	0.85	1.40
Compressor	0.85	1.37
Combustor	1.00[1]	1.35
Turbine	0.90	1.33
Nozzle	0.97	calc.[2]

(1) With 5% total pressure loss
(2) From internal mixing calculation

Table 2: Engine Characteristics at Supersonic Cruise
($y = 16000$ m, $M_\infty = 1.6$, $W = 480$ kN)

	B03-MIX	B30-SEP	B30-MIX
OPR	20	20	20
TIT (K)	1600	1800	1800
$\dot{m}_{\text{com}}$ (kg/s)	44	34	34
$\dot{m}_{\text{tot}}$ (kg/s)	57	89	89
$\mathcal{T}$ (kN)	24	24	24
BPR	0.3	3.0	3.0
FPR	4.5	2.25	2.25
$D_{\text{fan}}^{(2)}$(m)	0.93	1.44	1.44
TSFC (kg/kgf-h)	0.980	0.975	0.974[2]
M_p	2.06	1.54	1.75
U_p (m/s)	890	760	650
M_s	-	1.96	-
U_s (m/s)	-	610	-

(1) $M = 0.7$ at fan face
(2) Does not account for mixer losses

Table 3: Engine Characteristics at Takeoff
($y = 0$ m, $M_\infty = 0.3$, $W = 540$ kN)

	B03-MIX	B30-SEP	B30-MIX
OPR	20	20	20
TIT (K)	1800	2000	2000
$\dot{m}_{\text{com}}$ (kg/s)	120	94	94
$\dot{m}_{\text{tot}}$ (kg/s)	157	377	377
$\mathcal{T}$ (kN)	112	140	145
BPR	0.3	3.0	3.0
FPR	5.0	2.12	2.12
$D_{\text{fan}}^{(1)}$(m)	0.93	1.44	1.44
TSFC (kg/kgf-h)	0.778	0.587	0.565[2]
M_p	1.55	1.19	1.14
U_p (m/s)	770	700	490
M_s	-	1.12	-
U_s (m/s)	-	390	-

(1) $M = 0.5$ at fan face
(2) Does not account for mixer losses

hood of 1800°K, it is important to know what are the conditions that minimize fuel consumption. The overall pressure ratio (OPR), which for a supersonic engine should be in the range 15-25, has very slight effect on TSFC. The effects of bypass ratio (BPR) and fan pressure ratio (FPR) are shown in Figure 2, which plots iso-contours of TSFC on the BPR-FPR plane. The minimum TSFC occurs at BPR=2.2 and FPR=2.5. What is optimal for cruise, however, may not be the best choice for takeoff. A bypass ratio of 2.2 may be too small for quiet operation. In addition, fan pressure ratios above 2.4 will likely require a two-stage fan which complicates engine design. The selection here is an engine with BPR=3.0 and FPR=2.25. As seen in Fig. 2, this condition is very close to the optimum point yet increases significantly the chances for meeting noise regulations and affords the simplicity of a single-stage fan.

This study investigates the thermodynamic performance and noise emission from a "next generation" BPR=3.0 supersonic engine with a variety of exhaust arrangements. The exhaust configurations can be broken down into two broad classes, mixed-flow and separate-flow. For the separate-flow exhaust, nozzle arrangements will comprise coaxial, eccentric, and coaxial with deflectors in the bypass stream. A "current generation" supersonic turbofan engine is included in the comparisons in order to assess the improvements of the new concepts.

To size the engines, we consider a supersonic twin-engine aircraft with maximum takeoff weight of 540 kN (120,000 lb.) and wing loading of 4450 N/m^2 (100 lb/ft^2). The assumed lift-to-drag ratio is 5 at takeoff and 10 at supersonic cruise, values roughly 20% better than those of the Aerospatiale Concorde [5]. Weight at cruise is 480 kN, based on an average TSFC=0.6 kg/(kgf-hr) and a 20-min climb to cruise altitude.

The comparison basis is that all engines have the same cruise thrust at Mach 1.6 and altitude of 16000 m. On takeoff, the TIT is 200°K greater than the cruise setting while the OPR and FPR values are roughly the same as at cruise. The size, specific fuel consumption, and exhaust conditions are derived from thermodynamic analysis of a Brayton cycle with component efficiencies and specific heat ratios listed in Table 1 (see Ref. [7] for more information on the cycle analysis.) For all engines, 25-30% of the compressor air is used for turbine cooling; 1% of the compressor air is bled to systems outside the engine; and 1.5% of the turbine work drives auxiliary systems. Total pressure loss due to turbine cooling is estimated at 7% times the mass fraction of cooling air [6]. For the mixed-flow designs, the core and fan streams mix at constant pressure, constant total enthalpy, and Mach number 0.4 before expanding to ambient pressure.

Tables 2 and 3 summarize engine characteristics and thermodynamic performance at supersonic cruise and takeoff, respectively. For convenience, we adopt a notation that gives the bypass ratio and type of exhaust. B30-MIX, for example, describes the bypass ratio 3.0, mixed-flow engine. Because of its small bypass ratio, the "current generation" engine (B03-MIX) operates at much larger fan pressure ratio than the B30 variants. Increasing the bypass ratio from 0.3 ("current generation") to 3.0 ("next generation") produces a modest decrease in fuel consumption at supersonic cruise. There is hardly any difference between the fuel consumption of the separate-flow and mixed-flow B30 engines. In fact, the actual fuel consumption of B30-MIX may be slightly higher because of losses caused by the mixer. The velocity ratio of the separate-flow exhaust at cruise, $U_s/U_p = 0.80$, is very close to the efficiency of energy transfer between the core and bypass flows (the product of turbine and fan efficiencies, in this case 0.76). This indicates that B30-SEP operates near optimal cruise conditions [9].

On takeoff, the B30 engines produce substantially more thrust than does the low-bypass reference engine. The thrust-to-weight ratio is 0.5 for the B30-powered aircraft versus 0.4 for the reference case. The resulting initial climb angle,

$$\gamma \;=\; \arcsin\left(\frac{\mathcal{T}-D}{W}\right)$$

is 19° for the B30-powered aircraft versus 12° for the B03-powered aircraft and $\sim$ 15° for modern twin-engine subsonic aircraft. The steep climb angle gives the B30-powered aircraft an inherent noise advantage over the reference airplane.

Besides engine performance, important information that comes from the cycle analysis includes the exhaust velocities and Mach numbers on takeoff. These conditions are duplicated in subscale tests to assess the acoustics of each configuration.

Exhaust Configurations

Past research on high-speed jets has shown the powerful noise benefit of reshaping a dual-stream nozzle

from coaxial to eccentric [10]. Downward-directed Mach wave emission was reduced by the combination of two factors: shortening of the primary potential core (relative to the coaxial jet) and thickening of the secondary flow in the downward direction [11]. This synergism resulted in a reduction of the convective Mach number of flow instabilities that produce intense downward-radiated sound [4].

Very recent experiments have shown that the effect of the eccentric configuration can be achieved in a coaxial jet with deflectors placed in the bypass stream. The deflectors are small flaps, or vanes, that induce a slight downward tilt in the direction of the bypass stream. It is believed that this deflection scheme achieves two goals simultaneously: (a) creation of skewed mixing layers in the vicinity of the nozzle exit that enhance mixing and shorten the primary potential core; and (b) direction of most of the bypass stream to the lower side of the jet so that it shields the end of the potential core. For more details the reader is referred to Ref. [4].

Figure 3 shows exemplary illustrations of the separate-flow configurations considered for the B30 engines: coaxial; eccentric; and coaxial with vanes installed in the bypass stream. Figure 4 shows spark schlieren images that tend to support the hypothesis stated above about the effect of the vanes. The clean coaxial jet spreads very slowly. Insertion of vanes enhances mixing considerably and thickens the bypass stream on the underside of the jet. The deflectors produce superior noise reduction compared to the eccentricity method. Applied to an engine, they could be actively deflected or deployed, confining any thrust losses to the takeoff and landing segments only.

Facilities and Flow Conditions

Noise testing was conducted in UCI's Jet Aeroacoustics Facility [10]. Single- and dual-stream jets with flow conditions matching those given by the cycle analysis (Table 3) were produced. The jets were composed of helium-air mixtures, which duplicate very accurately the fluid mechanics and acoustics of hot jets [12]. Jet nozzles were fabricated from epoxy resin using rapid-prototyping techniques. The nozzles of BO3-MIX and B30-MIX cases were designed with the method of characteristics for Mach numbers 1.5 and 1.2, respectively. For the separate-flow configurations, the primary nozzle was convergent, terminating in a constant-area section, and had a plug along its centerline. All primary nozzles had the same exit inner diameter (14.8 mm), lip thickness (0.7 mm), and external shape. The plug diameter was 10.0 mm. One secondary (bypass) nozzle formed a convergent duct in combination with the primary nozzles and terminated in a diameter of 21.8 mm. The pipe that fed the primary nozzle was able to flex, enabling coaxial or eccentric secondary flow passages. For all nozzles, the radial coordinates of the contraction (prior to any supersonic expansion) were given by fifth-order polynomials. The contraction ratio was 4:1 for the core nozzles (8:1 with the plug inserted) and 15:1 for the bypass nozzle. The jet Reynolds number was on the order of 0.5×10^6. Table 1 summarizes the flow conditions.

Figure 5 shows a picture of the B30 nozzle with deflectors attached. The outer wall of the core nozzle extended past the exit of the bypass nozzle. Four vanes, made of thin metal sheet, were attached on the outer wall of the core nozzle immediately past the exit of the bypass nozzle. With $\phi = 0$ indicating the downward vertical direction, the vanes were placed at azimuth angles $\phi = \pm 80^\circ$ and $\pm 110^\circ$. The vane angle of attack was approximately 20°. The size of each vane was 4 mm in chord by 1.7 mm in width. The width was 40% smaller than the annulus thickness of the bypass duct. The forces on the vanes were calculated from basic aerodynamic relations [17]. Each vane was treated as a wing with aspect ratio equal to twice the width divided by the chord length. The two dimensional lift slope was assumed to be 0.1/deg and the parasite drag coefficient was assumed to be 0.01. Because of the small aspect ratio, the three-dimensional lift slope is quite small (around 0.04 /deg), allowing deflections up to about 25° without exceeding a lift coefficient of 1.0. It is expected, therefore, that the vanes are not stalled even at such high angle of attack.

Noise measurements were conducted inside an anechoic chamber using a one-eighth inch condenser microphone (Brüel & Kjær 4138) with frequency response of 140 kHz. The microphone was mounted on a pivot arm and traced a circular arc centered at the jet exit with radius of 70-100 core diameters. Earlier experiments have determined that this distance is well inside the acoustic far field [13]. Figure 6 depicts the overall setup and the range of polar angles covered. The sound spectra were corrected for the microphone frequency response, free field response, and atmospheric absorption. Comparison at equal thrust was done using geometric scaling [13].

Table 1: Flow Conditions

Test	Configuration	D_p (mm)	U_p (m/s)	M_p	D_s (mm)	U_s (m/s)	M_s	F_x^{**}	F_y^{**}
B30-MIX	Mixed flow	14.4	490	1.14	-	-	-	0.0%	0.0%
B30-COAX	Coaxial (clean)	10.0*	700	1.19	21.8	390	1.12	0.0%	0.0%
B30-ECC	Eccentric	10.0*	700	1.19	21.8	390	1.12	Unknown	Unknown
B30-4V20e	Coaxial with four vanes inclined 20°, ext. to bypass duct	10.0*	700	1.19	21.8	390	1.12	1.7%	5.0%
B03-MIX	Mixed flow (ref.)	14.4	770	1.55	-	-	-	0.0%	0.0%

* This is the effective (area-based) diameter of the primary nozzle. Actual dimensions are 14.4 mm ID with a 10-mm plug.

** F_x and F_y are estimates of the axial and transverse forces, respectively, caused by the nozzle modifications. They are presented in percent of total thrust.

Spectra and OASPL

This section discusses the absolute noise levels (spectra and OASPL) recorded in the lab. Only the B30 variants are compared–the B03 case is covered in the perceived noise section.

Sound pressure level spectra are scaled up to full engine size and referenced to equal thrust. Figure 7a compares the spectra in the direction of peak emission of the B30 separate-flow variants. For the low-to-mid frequencies, the eccentric jet is 5 dB quieter than the clean coaxial jet while the coaxial jet with vanes in the bypass exhaust is 10 dB quieter than the clean coaxial jet. The exhaust with vanes maintains a substantial advantage, around 10 dB, when compared to the mixed-flow exhaust, as shown in Fig. 7b. In the lateral direction, Fig. 8, the exhaust with vanes is 1-2 dB quieter than the coaxial or eccentric jets and 1-2 dB louder than the mixed-flow configuration.

Figure 9 compares the directivity of OASPL at constant thrust and fixed radius from the jet exit for all the B30 variants. The advantage of B30-4V20e is again evident: it reduces the peak OASPL by 8 dB relative to the mixed-flow exhaust and by 6 dB relative to the coaxial exhaust. The eccentric arrangement also produces a significant noise benefit, but it is about 2 dB less than the benefit of the coaxial exhaust with vanes in the bypass stream. The overall trends produced by the eccentric and vane configurations bear a striking resemblance to the effect of forward flight on OASPL [14]. This is not believed to be coincidental. The eccentric and vane arrangements create an effect similar to that of forward flight, that is, reduction of the convective Mach number of large-scale instabilities [4].

Perceived Noise Level

This section describes the procedures for estimating the perceived noise level of aircraft powered by the various engines. We calculate noise recorded from the takeoff monitor for a full-power takeoff. Future studies will address takeoff with power cutback and noise recorded by the sideline and approach monitors.

Flight Path

The first step in assessing perceived noise is definition of the takeoff flight path and attitude of the engines relative to the flight path. The airplanes are those defined in the Engine Cycle section, i.e., twin-engine with thrust given by the specifications of Table 3. All aircraft must have the same weight as they share the same cruise thrust. The flight path of the B30-powered aircraft comprises a takeoff roll $x_{\text{LO}} = 1500$ m followed by a straight climb at angle $\gamma = 19°$. The reference B03-powered airplane lifts off at $x_{\text{LO}} = 2000$ m and climbs at $\gamma = 12°$. For all aircraft, the lift coefficient at climb is 0.6, which for a delta-wing aircraft corresponds to an angle of attack $\alpha = 12°$ [16]. The engine exhaust axis is assumed to be inclined at the angle of attack. Figure 10 shows the generic flight path with key variables.

The takeoff flight speed of all airplanes is 110 m/s ($M_\infty = 0.32$). The cartesian position (x, y) of the airplane is calculated at 0.5-sec intervals from the time of lift off. For each aircraft location, its polar coordinates (r, ψ) relative to the flight path and seen by the takeoff monitor are calculated. Here we distinguish between the apparent (r', ψ') and true (r, ψ) locations of the airplane with regard to sound

emission. The apparent location is the actual location of the airplane. The true location is the one from which sound reached the observer. It is easily shown that the true position is at a distance $M_\infty r$ behind the apparent position along the flight path. From the geometry of Fig. 10, the apparent coordinates are

$$r' = \sqrt{y^2 + (x - x_{\text{TOM}})^2}$$

$$\psi' = \frac{\pi}{2} - \gamma - \arctan\left(\frac{x - x_{\text{TOM}}}{y}\right)$$

and the true coordinates are obtained from

$$r = \frac{r'}{1 - M_\infty^2}\left[-M_\infty \cos\psi' + \sqrt{1 - M_\infty^2 \sin^2\psi'}\right]$$

$$\sin\psi = \frac{r'}{r}\sin\psi'$$

The polar angle of the exhaust observed by the takeoff monitor is

$$\theta = \psi - \alpha$$

Using these relations, the true distance r and emission angle θ are obtained as functions of time observed by the takeoff monitor.

Data Processing

Following are the steps for processing the laboratory narrowband spectra into perceived noise level:

1. The spectra are corrected to zero absorption using the relations of Bass et al. [18].

2. The spectra are extrapolated to frequencies higher than those resolved in the experiment (140 kHz) using a decay slope of -30 dB/decade. This is done to resolve the audible spectrum for a full-scale engine. The PNL results are very insensitive on the assumed slope.

3. The spectra are scaled up to engine size by dividing the laboratory frequencies by the scale factor $\sqrt{\mathcal{T}_{\text{eng}}/\mathcal{T}_{\text{exp}}}$. The full-scale engine diameter is the experimental diameter multiplied by this scale factor.

4. The spectra are Doppler-shifted to account for the motion of the aircraft. The relations of McGowan & Larson [19] are used. In those relations, the value of the convective Mach number M_c is obtained from the empirical relations of Murakami & Papamoschou [20].

5. For each observation time t, the scaled-up spectrum corresponding to $\theta(t)$ is obtained. This step requires interpolation between spectra and, for angles outside the range covered in the experiment, moderate extrapolation. To enhance the accuracy of interpolation or extrapolation the spectra are smoothed to remove their wiggles.

6. For each t, the corresponding scaled-up spectrum is corrected for distance and atmospheric absorption. The distance correction is

$$-20\log_{10}\left[\frac{(r/D_p)_{\text{eng}}}{(r/D_p)_{\text{exp}}}\right]$$

   The absorption correction is applied for ambient temperature 29°C and relative humidity 70% (conditions of least absorption) using the relations of Bass et al. [18].

7. For each t, the corresponding scaled-up, corrected spectrum is discretized into 1/3-octave bands. The perceived noise level (PNL) is then computed according to Part 36 of the Federal Aviation Regulations [15].

8. The previous step gives the time history of perceived noise level, PNL(t). From it, the maximum level of PNL, PNLM, is determined. The duration of PNL exceeding PNLM-10 dB is calculated and the corresponding "duration correction" is computed according to FAR 36. The effective perceived noise level, EPNL, equals PNLM plus the duration correction. The estimate of EPNL does not include the "tone correction", a penalty for excessively protrusive tones in the 1/3-octave spectrum.

Results

Figure 11 compares the PNL time histories of aircraft powered by the B30 engine variants. The superiority of the coaxial exhaust with vanes in the bypass exhaust is evident. It lowers the peak PNL by 6 dB and reduces the PNLM-10 time by 20%. EPNL is as follows: 97.5 dB for B30-MIX; 95.5 dB for B30-COAX; 92.0 dB for B30-ECC; and 90.5 dB for B30-4V20e. In other words, the coaxial exhaust with vanes produces an 7-dB benefit in EPNL over the mixed-flow exhaust. Note that the EPNL numbers presented here do not capture the effect of forward flight. It is expected that all the EPNL values will drop with increasing flight Mach number and

that the gap between B30-MIX and B30-4V20e will widen [4].

To get an idea of the improvement over "current generation" engines, Fig. 12 plots the PNL time history of an aircraft powered by the reference B03-MIX engine and an aircraft powered by the B30-4V20E engine. Recall that the two aircraft have difference takeoff performance: the one powered by the larger-bypass engine lifts off sooner and climbs at 19° versus 12° for the reference airplane. The increase in bypass ratio, combined with the new exhaust configuration, gives a 20-EPNdB noise reduction. This is the ballpark figure cited in numerous studies for bringing noise emission of supersonic aircraft on a par with subsonic aircraft. Note that the traditional exhaust configuration (B30-MIX) produces only a 13-dB benefit relative to the reference case.

Assessment of Noise Reduction

Given that its is difficult to make absolute EPNL predictions due to lack of the forward-flight effect, it is instructive to estimate the *equivalent* exhaust velocity of B30-4V20e as far as noise emission is concerned. To this end, Fig. 13a plots the peak OASPL (scaled to equal thrust and fixed distance from the jet) versus specific thrust of single-stream jets investigated over a period of time in our facility. Overlaid on the plot is the datum of B30-4V20e. The single-jet data follow very well the V^8 law up to a velocity of 600 m/s, beyond which the growth exponent declines rapidly. Extrapolating the V^8 trend to the OASPL level of B30-4V20e, one finds that the single-stream jet that produces the same noise as B30-4V20e has a velocity of 380 m/s. The effect of the vanes, therefore, was to reduce the noise-equivalent specific thrust from 490 m/s to 380 m/s. Fig. 13b does an analogous comparison in terms of EPNL and leads to a very similar result: the noise-equivalent velocity of the jet is 390 m/s. The exhaust speed range of 380-390 m/s is representative of that found in high-bypass turbofan engines powering subsonic commercial aircraft.

Most importantly, the plots of Fig. 13 illustrate the basic philosophy and paradigm shift of the approach proposed here: suppression of noise via reduction of the convective Mach number while maintaining a relatively high exhaust speed.

Concluding Remarks

The experiments presented in this paper demonstrate that it is possible to reduce jet noise significantly while maintaining a high specific thrust. This should help development of turbofan engines that are quiet on takeoff and efficient at supersonic cruise. The principle of noise suppression is reduction of the convective Mach number of the turbulent eddies that cause intense downward radiation: the more subsonic the eddies become, the less noise is radiated to the far field. To achieve this, present experience indicates the requirement of two conditions: mixing enhancement of the core flow and thickening of the bypass stream on the underside of the jet.

The preferred implementation of this approach entails installation of vanes in the exhaust of the bypass stream of a separate-flow turbofan engine. The vanes give a slight downward direction to the bypass flow (relative to the core flow) and create locally-skewed mixing layers between the core stream and the bypass stream. Large reductions in downward-emitted actual and perceived noise, about 7-8 dB, were measured relative to the mixed-flow exhaust. The vanes can be fixed of variable. With a variable geometry, thrust losses (which are estimated on the order of 1-2%) would be confined to the noise-sensitive segments of flight only.

The preliminary cycle analysis presented in this paper shows that even a BPR=3.0 supersonic engine would have trouble meeting noise regulations without some kind of suppression scheme. The supersonic cruise requirements lead to an engine with high specific thrust on takeoff, in this case 490 m/s. Implementation of vanes as noted above reduces the noise-equivalent specific thrust (in terms of OASPL or EPNL) to the range of 380-390 m/s. Compliance with noise restrictions would thus be greatly facilitated. In addition, the inherently fast climb of a BPR=3 powered supersonic airplane will increase the noise compliance margin.

A lot of work remains to be done on optimization of the deflection scheme and characterization of the basic flow phenomena. The promising results of this exploratory work suggest that significant improvements in noise emission can be achieved with relatively simple and efficient modifications of the exhaust.

Special Notice

The method and apparatus of noise suppression via deflection of the bypass and/or core streams is proprietary to the University of California. U.S. Patent Pending.

Acknowledgments

The support by NASA Glenn Research Center is gratefully acknowledged (Grant NAG-3-2345 monitored by Dr. Khairul B. Zaman). Ms. Erin Abbey is thanked for her work on nozzle design.

References

[1] Smith, M.J.T., "Aircraft Noise", 1st Ed., Cambridge University Press, 1989, pp. 120-134.

[2] Tillman, T.G., Paterson, R.W., and Presz, W.M., "Supersonic Nozzle Mixer Ejector", *AIAA Journal of Propulsion and Power*, Vol. 8, No. 2, 1992, pp. 513-519.

[3] Papamoschou, D. and Debiasi, M., "Mach Wave Elimination Applied to Turbofan Engines," AIAA-2002-0368.

[4] Papamoschou, D., "Noise Suppression in Moderate-Speed Multistream Jets," AIAA-2002-2557.

[5] Mair, W.A. and Birdsall, D.L., "Aircraft Performance," 1st Ed., Cambridge Aerospace Series 5, 1992, pp. 260-261.

[6] Horlock, J.H., Watson, D.T., and Jones, T.V., "Limitations on Gas Turbine Performance Imposed by Large Turbine Cooling Flows," *Journal of Engineering for Gas Turbines and Power*," Vol. 123, July 2001, pp. 487-494.

[7] Debiasi, M., and Papamoschou, D., "Cycle Analysis for Quieter Supersonic Turbofan Engines," AIAA-2001-3749.

[8] Lord, W.K., MacMartin, D.G., and Tillman, T.G., "Flow Control Opportunities in Gas Turbine Engines," AIAA-2000-2234.

[9] Guha, A. "Optimum Fan Pressure Ratio for Bypass Engines with Separate or Mixed Flow Exhaust Streams," *AIAA Journal of Propulsion and Power,* Vol. 17, No. 5, 2001, pp. 1117-1122.

[10] Papamoschou, D., and Debiasi, M., "Directional Suppression of Noise from a High-Speed Jet," *AIAA Journal*, Vol. 39, No. 3, 2001, pp. 380-387.

[11] Murakami, E., and Papamoschou, D. "Mean Flow Development of Dual-Stream Compressible Jets," *AIAA Journal*, Vol. 40, No. 6, 2002, pp. 1131-1138.

[12] Kinzie, K.W., and McLaughlin, D.K., "Measurements of Supersonic Helium/Air Mixture Jets," *AIAA Journal,* Vol. 37, No. 11, 1999, pp. 1363-1369.

[13] Papamoschou, D., and Debiasi, M. "Noise Measurements in Supersonic Jets Treated with the Mach Wave Elimination Method," *AIAA Journal*, Vol. 37, No. 2, 1999, pp. 154-160.

[14] Hoch, R.G. and Berthelot, M., "Use of the Bertin Aerotrain for the Investigation of Flight Effects on Aircraft Engine Exhaust Noise," *Journal of Sound and Vibration,* Vol. 54, No. 2, 1977, pp. 153-172.

[15] Federal Aviation Regulations Part 36 - Noise Standards: Aircraft Type and Airwowrthiness Certificiation.

[16] Bertin, J.J. and Smith, M.L., "Aerodynamics for Engineers," 3rd Ed., Prentice Hall, 1998, pp. 319-321.

[17] Shevell, R.S., "Fundamentals of Flight," Prentice Hall, 1989, pp. 265, 293.

[18] Bass, H.E., Sutherland, L.C., Zuckerwar, A.J., Blackstock, D.T., and Hester, D.M., "Atmospheric Absorption of Sound: Further Developments, " *Journal of the Acoustical Society of America,* Vol. 97, 1995, pp. 680-683.

[19] McGowan, R.S. and Larson, R.S., "Relationship Between Static, Flight and Simulated Flight Jet Noise Measurements," *AIAA Journal*, Vol. 22, No. 4, 1984, pp. 460-464.

[20] Murakami, E., and Papamoschou, D., " Eddy Convection in Supersonic Coaxial Jets," *AIAA Journal*, Vol. 38, No.4, 2000, pp. 628-635.

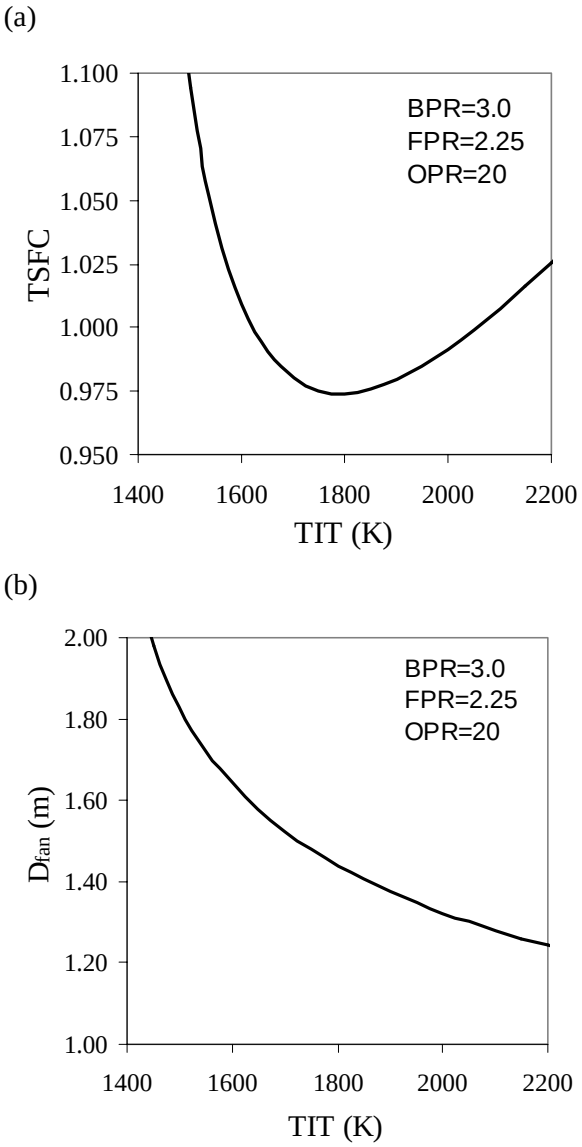

Fig.1 Variation of (a) thrust specific fuel consumption and (b) fan diameter with turbine inlet temperature for an engine developing 24 kN of thrust at flight Mach number 1.6.

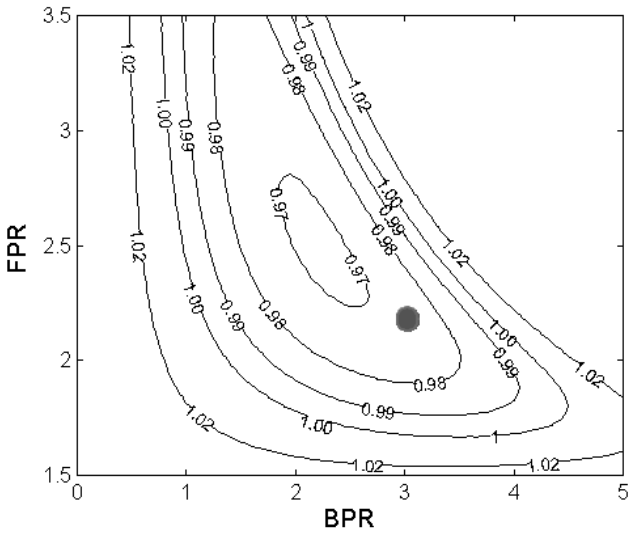

Fig.2 Isocontours of TSFC on the BPR-FPR plane for $M_\infty = 1.6$. TIT=1800° and OPR=20. Dot indicates current design.

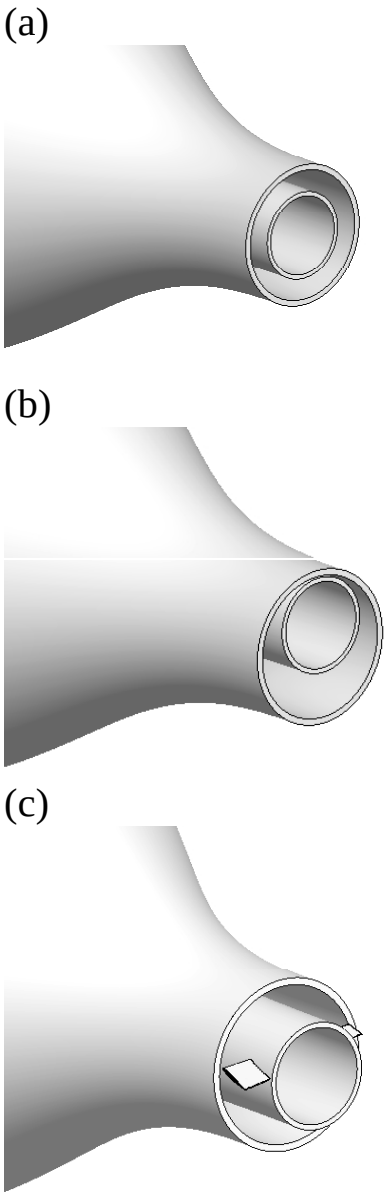

Fig.3 Exemplary illustrations of the separate-flow exhaust configurations considered in this study: (a) clean coaxial; (b) eccentric; and (c) coaxial with bypass deflectors.

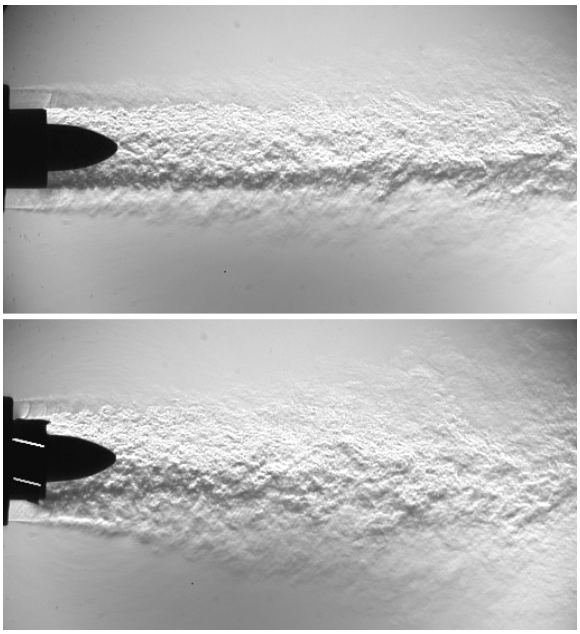

Fig.4 Schlieren images of exhaust flow. Upper: clean coaxial nozzle. Lower: coaxial nozzle with four vanes installed immediately downstream of the bypass duct. From Ref. [4].

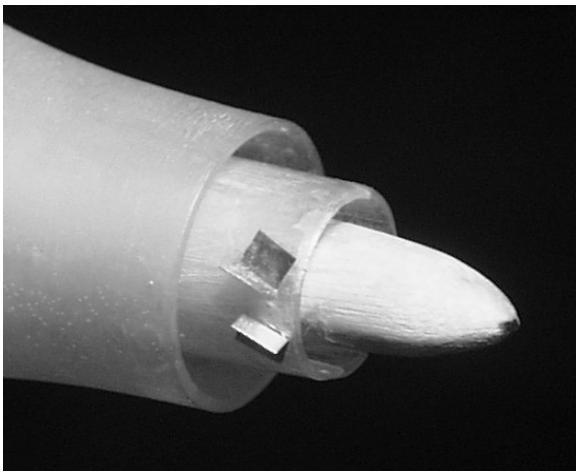

Fig.5 Picture of nozzle B30-4V20e.

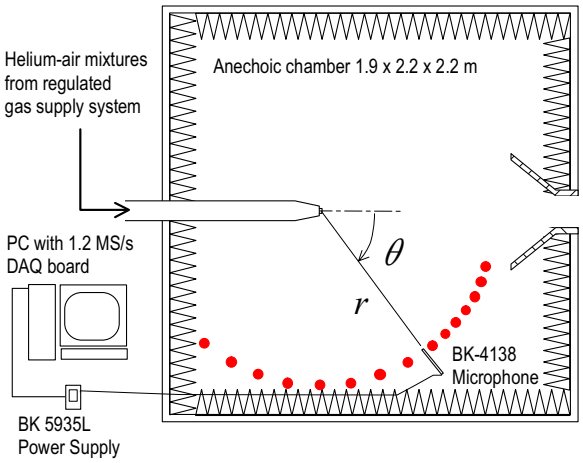

Fig.6 Experimental setup with set of polar angles covered.

(a)

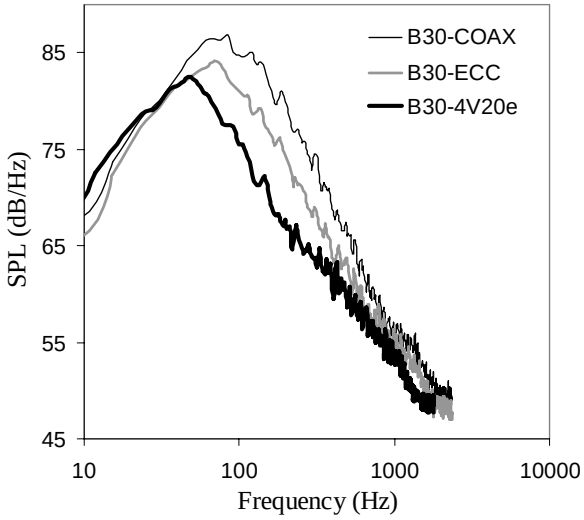

(b)

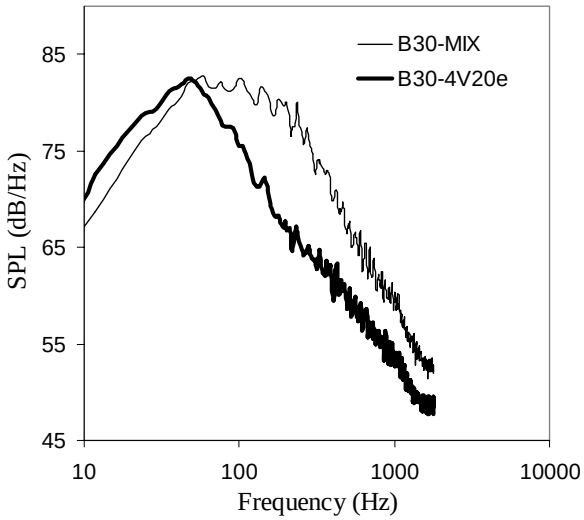

Fig.7 Far-field, scaled-up spectra in the direction of peak emission ($\theta = 30°$) for the B30 variants. (a) Comparison among the separate-flow variants; (b) comparison between B30-4V20e and B30-MIX.

(a)

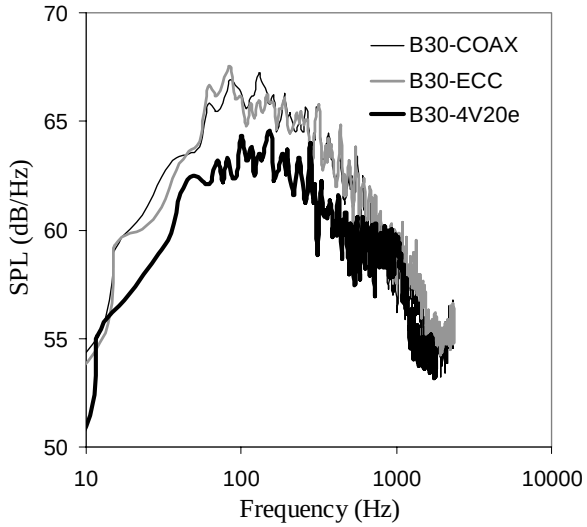

(b)

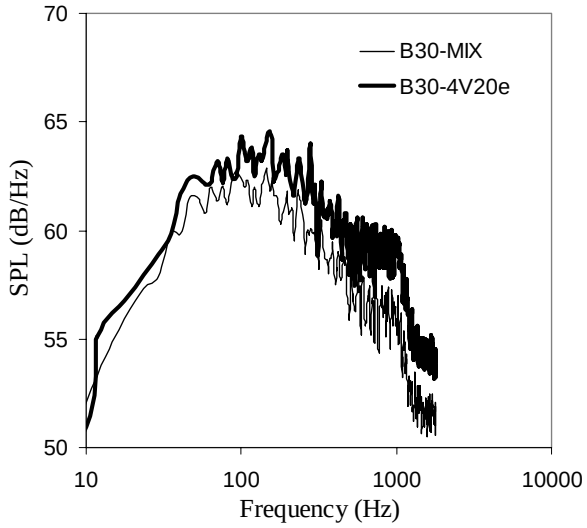

Fig.8 Far-field, scaled-up spectra in the lateral direction ($\theta = 90°$) for the B30 variants. (a) Comparison among the separate-flow variants; (b) comparison between B30-4V20e and B30-MIX.

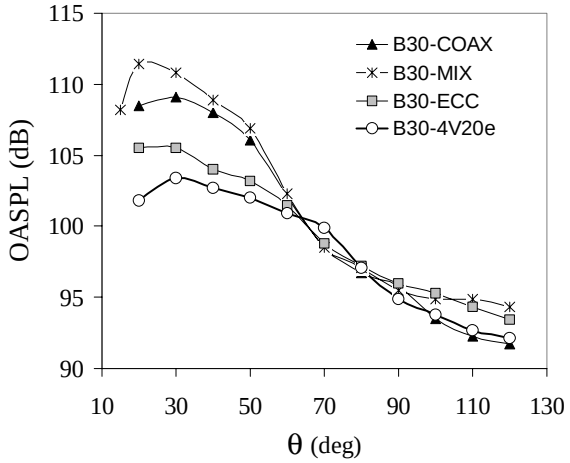

Fig.9 Directivity of overall sound pressure level for the B30 variants.

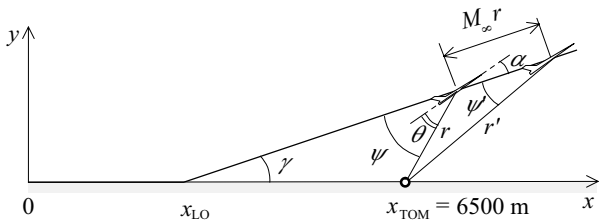

Fig.10 Flight path used for estimating perceived noise level.

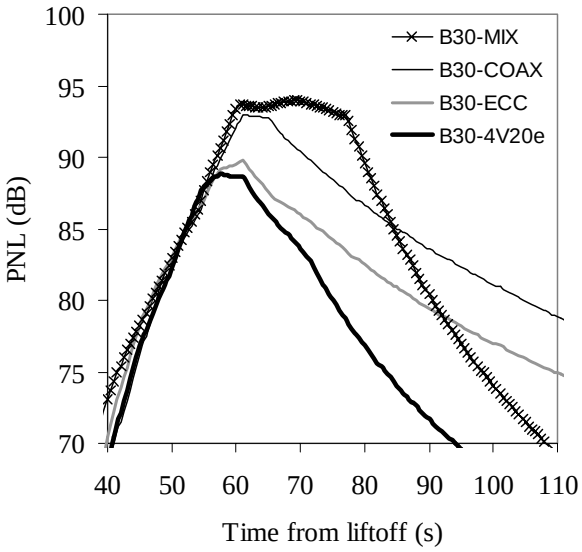

Fig.11 Time history of flyover perceived noise level (PNL) of aircraft powered by the B30 variants.

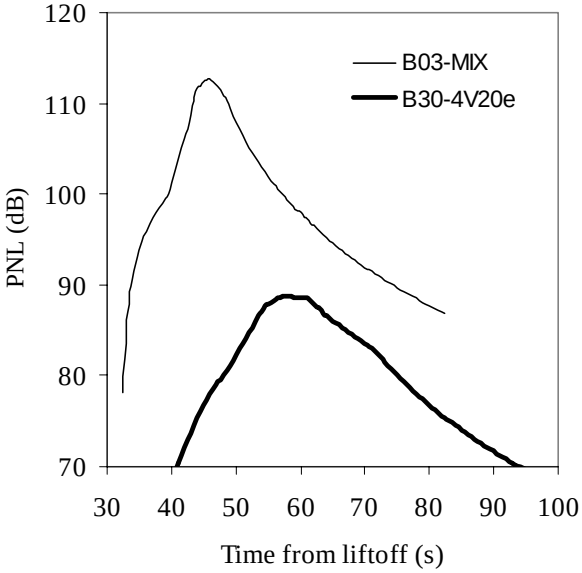

Fig.12 Time history of flyover perceived noise level for aircraft powered by B03-MIX and B30-4V20e.

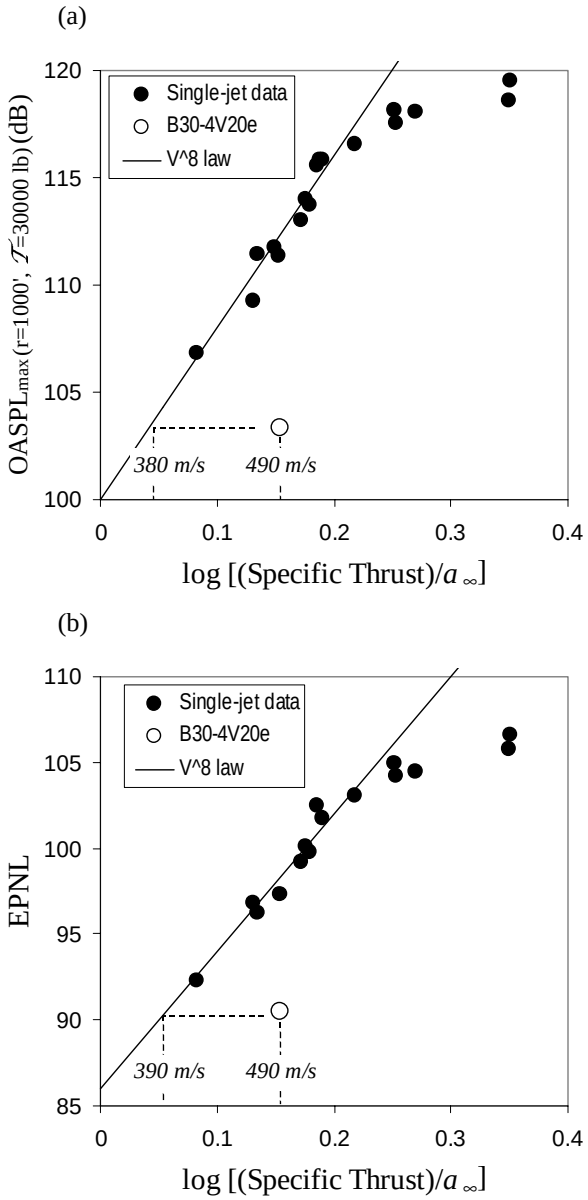

Fig.13 Comparison of the noise emission of B30-4V20e with that of single-stream jets. (a) OASPL; (b) EPNL.